Molecular Dissection of Neural Circuits Controlling Nicotine Aversion

Silke Frahm, PhD; Marta A. Slimak;
Julio Santos-Torres, PhD;
Beatriz Antolin-Fontes; Sebastian Auer, PhD;
and Inés Ibañez-Tallon, PhD

Department of Molecular Neurobiology
Max Delbrück Center for Molecular Medicine
Berlin, Germany

NOTES

Introduction

Tobacco use is a major public health challenge leading to millions of preventable deaths every year (http://www.who.int/tobacco/statistics/tobacco_atlas/en/). The principal addictive component of tobacco is the plant alkaloid nicotine, which binds and activates nicotinic acetylcholine receptors (nAChRs) (Dani and Heinemann, 1996). In the mammalian nervous system, eight alpha (α2–α7 and α9–α10) and three beta (β2–β4) subunits assemble into pentameric nAChR combinations with distinctive pharmacological and functional properties (McGehee and Role, 1995; Gotti et al., 2009). Recently, genome-wide association studies (GWAS) have identified genetic variants in the *Chrnb4–CHRNA3–CHRNA5* gene cluster as risk factors for nicotine dependence and lung cancer (Thorgeirsson et al., 2008; Weiss et al., 2008; Saccone et al., 2009; Amos et al., 2010a). These single nucleotide polymorphisms (SNPs) include noncoding variants across the gene cluster, as well as amino acid substitutions (http://www.ncbi.nlm.nih.gov/snp/). Given that *cis*-regulatory elements within the cluster coordinate transcription of these genes for assembly of α3β4-containing (α3β4*) and α3β4α5 functional nAChRs (Xu et al., 2006; Scofield et al., 2010), the fact that a large number of SNPs map to noncoding segments of the cluster suggests that altered regulation of these genes can contribute to the pathophysiology of tobacco use. Indeed, the risk for nicotine dependence seems to stem from at least two separate mechanisms: the variability in the mRNA levels of these genes and functional changes due to nonsynonymous amino acid variants (Lu et al., 2009).

A number of mouse models with gene deletions, point mutations, or strain-specific variants in nAChR subunits have been critical to elucidating the role of the different nAChR combinations in nicotine addiction and withdrawal. For instance, α4β2 nAChRs (accounting for 80% of the high-affinity nicotine binding sites in the brain) (Whiting and Lindstrom, 1988) are major contributors to nicotine self-administration, as shown in β2 knock-out (KO) mice (Picciotto, 1998; Maskos et al., 2005) and in knock-in mice with a gain-of-function mutation of α4 (Tapper et al., 2004). The nAChR β4 subunit is almost always coexpressed with α3, while the auxiliary α5 subunit assembles with the α3β4 combination but can also be incorporated into α4β2 receptor complexes. The expression of the α3β4* nAChR combination is restricted to a few discrete brain areas, including the medial habenula (mHb) and interpeduncular nucleus (IPN), and to autonomic ganglia (Zoli et al., 1995). α3β4* nAChRs have a lower affinity for nicotine than α4β2 receptors and are likely less desensitized at the nicotine levels found in smokers than α4β2 nAChRs. This suggests that α3β4* nAChRs could play an important role in tobacco addiction, since they retain their sensitivity to fluctuating nicotine levels in smokers (Rose, 2007). β4 and α5 KO mice show similar phenotypes, including decreased signs of nicotine withdrawal symptoms (Jackson et al., 2008; Salas et al., 2004, 2009), hypolocomotion, and resistance to nicotine-induced seizures (Kedmi et al., 2004; Salas et al., 2004). It has been more difficult to assess the role of α3* nAChRs because KO mice die within 3 weeks after birth owing to severe bladder dysfunction (Xu et al., 1999).

Here we show that α3β4α5 nicotinic acetylcholine receptor activity *in vitro* and *in vivo* is limited by the level of *Chrnb4* expression and that the ability of the β4 subunit to increase α3β4α5 currents depends on a single, unique residue (S435). This residue maps to the intracellular vestibule of the nAChR complex adjacent to the rs16969968 SNP in *CHRNA5* (D398N), which has been linked to a high risk of developing nicotine dependence in humans. We present a novel transgenic mouse model of the *Chrnb4–Chrna3–Chrna5* gene cluster, referred to as Tabac (Transgenic a3b4a5 cluster) mice. In these mice, *Chrnb4* overexpression enhances α3β4* nAChR levels, resulting in altered nicotine consumption and nicotine-conditioned place aversion. Lentiviral vector–mediated transduction of the mHb of Tabac mice with the D398N *Chrna5* variant reversed the nicotine aversion induced by β4 overexpression. This study provides a new mouse model for nicotine dependence, demonstrates a critical role for the mHb in the circuitry controlling nicotine consumption, and elucidates novel molecular mechanisms that contribute to these phenotypes.

Results

The relative levels of α5 and β4 subunits strongly affect α3β4α5 nAChR currents

Recently, it has been shown that α5 competes with β4 for association with α4, and that this competition does not occur if β4 is substituted by β2 (Gahring and Rogers, 2010). The *CHRNB4–A3–A5* gene cluster regulates the co-expression of β4, α3 and α5 subunits, and SNPs in the regulatory regions of the cluster, as well as non-synonymous variants such as rs16969968 (corresponding to D398N in *CHRNA5*), associated with nicotine

NOTES

dependence (Bierut et al., 2008; Saccone et al., 2009; Beirut, 2010). Given these evidences, we were first interested in determining whether varying the relative expression levels of α3, β4, and α5 (wild type and D398N) subunits influences nicotine-evoked currents.

To measure this effect, we performed electrophysiological recordings in oocytes injected with cRNA transcripts of the different mouse subunits. In these experiments (Fig. 1), the cRNA concentration of α3 was held constant (1 ng/oocyte), whereas the concentration of β4 or β2 input cRNA varied from 1, 2, 4, 5 to 10 ng, respectively. These experiments showed that β4, but not β2, was able to increase current amplitudes in a dose-dependent manner (Fig. 1*A*,*B*). Next we held constant the concentrations of α3 and β4 at 1:10 and added the cRNA of α5 wild type (Wt) or the α5 D397N variant (corresponding to the human α5 variant D398N) at ratios of 1:10:1, 1:10:5 and 1:10:10 (Fig. 1*A*). We observed a significant decrease of current amplitudes at higher concentrations of α5, and this effect was significantly more pronounced with α5 D397N. These results suggest that α5 and β4 may compete for binding to α3, in line with the studies showing such competition for binding to α4 (Gahring and Rogers, 2010).

Given that overexpression of β2 with either α3 (Fig. 1*A*) or α4 (data not shown) did not increase currents, we were interested in identifying the residues differing between β4 and β2 that mediate this effect. Since the long cytoplasmic loop is the most divergent domain between nAChR subunits, and since it has been implicated in cell-surface expression and trafficking of β2 subunits (Nashmi et al., 2003; Ren et al., 2005), we generated β2–β4 chimeras exchanging either this domain, or short motifs and single residues within this domain. Replacement of the cytoplasmic loop of β2 with the corresponding sequences present in β4 (β2/β4 322–496) led to a strong increase of nicotinic currents (Fig. 1*C*). Introducing two β4-specific motifs: a serine/tyrosine rich motif (β2/+β4 382–391) and gephyrin-like binding motif (β2/+β4 401–419) into the β2 loop had no influence on current amplitudes (Fig. 1*C*).

We next performed bioinformatic analyses and singled out eight β4-specific residues (indicated as T-1 to T-8 in supplemental Fig. S1*C*) present within highly conserved motifs. Six of these residues were not further considered: T-2, T-3, T-6, and T-7 residues differ between mouse and chicken β4 subunits, which are equally potent in enhancing nicotine-evoked currents (Fig. S1*B*); T-4 residue lies within the tested motif in the β2/+β4 382–391 chimera; and residues at position T-8 have the same charge (Fig. S1*C*). The remaining two candidates, T-1 (S324 in β4 and T327 in β2) and T-7 (S435 in β4 and R431 in β2) (Fig. S1*C*), were tested by point mutagenesis in the β2 subunit backbone. The β2 T327S point mutant did not increase current, whereas replacement of β2 R431 with serine resulted in a 3.5-fold current increase (Fig. 1*C*). Furthermore, point mutation of the native S435 in the β4 subunit to the arginine residue present in β2 (β4 S435R) abolished the β4-specific activity. Thus, these data demonstrate that the distinctive ability of β4 to increase currents when overexpressed maps to a single residue (S435). This residue is both required in β4 for current increase and can confer this property to β2.

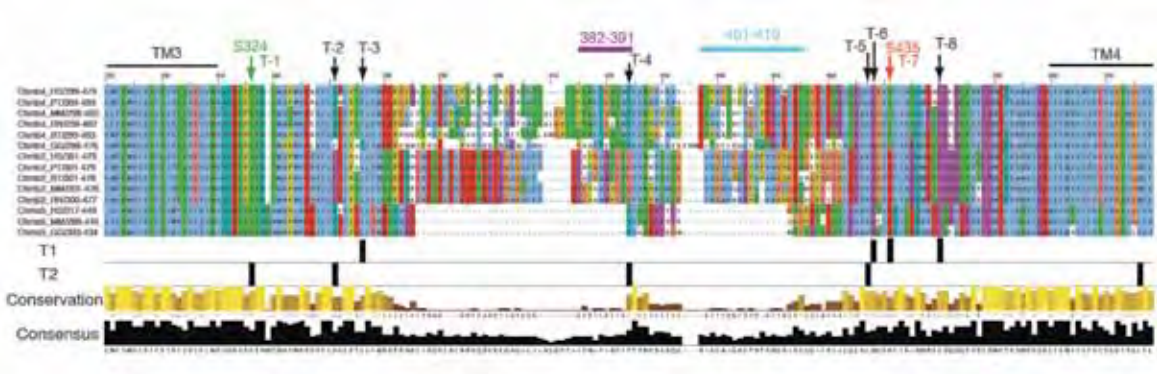

Supplemental Figure 1. Alignment of Chrnb4, Chrnb2, and Chrna5 protein sequences from different species reveals single differential amino acids within highly conserved regions. A custom track T β4/β2,α5 shows the differential conservation scores of β4 sequences compared with β2 and α5 (the resulting differential residues were designated T-3 and T-6-8). T β4/β2,α5 shows the differential conservation scores of β2 sequences compared to β4 and α5 (the resulting differential residues were designated T-1-2 and T-4-5). The tracks below show the global conservation and the consensus residues. Two residues of β4 (S324 and S435, green and red arrows) showing differential conservation score were selected for generation of β2- β4 chimeras shown in Figure 5*D*. HS, *Homo sapiens*; PT, *Pan troglodytes*; MM, *Mus musculus*; RN, *Rattus norvegicus*; BT, *Bos taurus*; GG, *Gallus gallus*; TM, transmembrane domain.

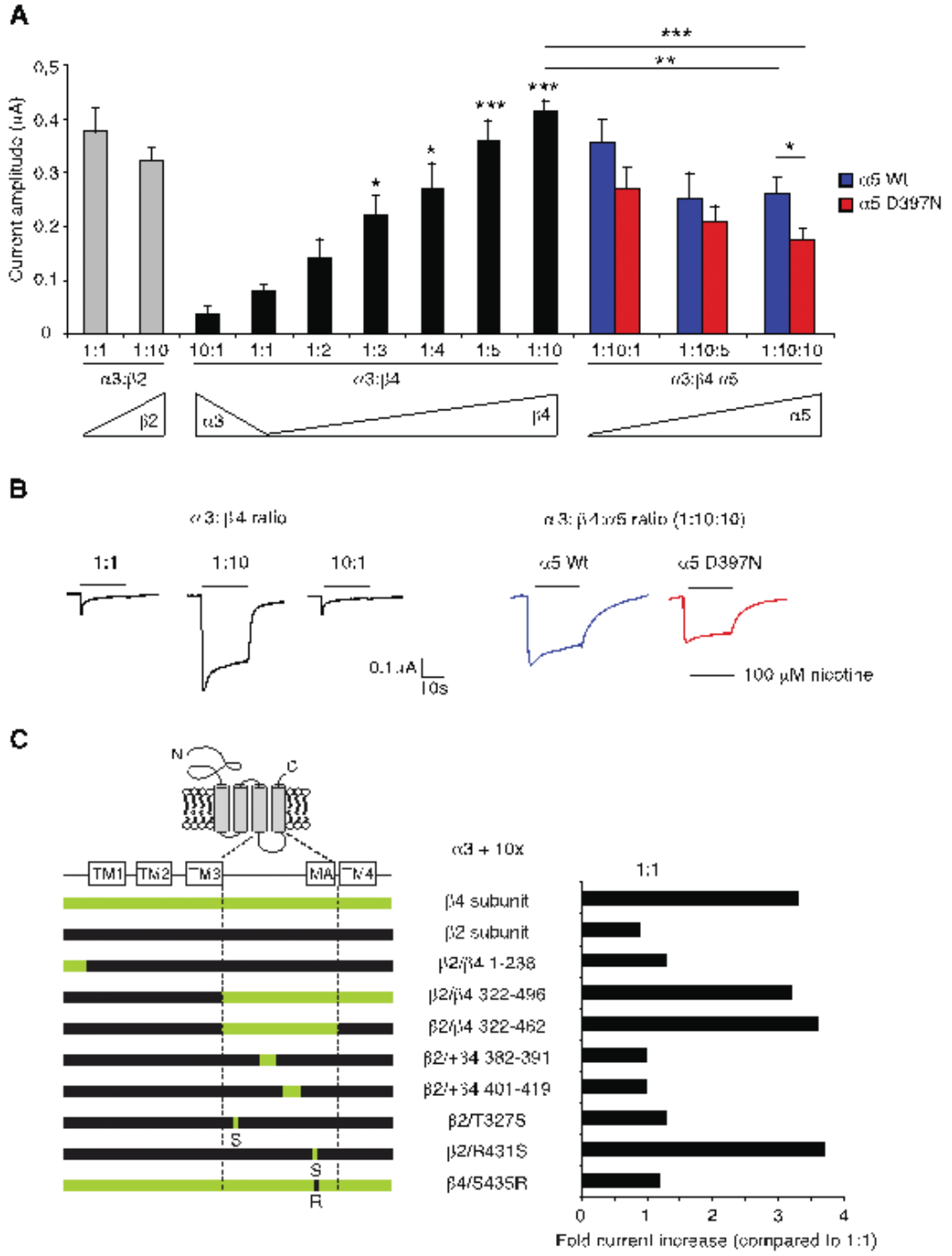

Figure 1. Increase of nAChR currents by β4 is competed by α5 and maps to a single amino acid (S435). ***A***, Quantification of nicotine-evoked currents (100 μM, 20 s) recorded in *Xenopus* oocytes injected with mouse α3:β2, α3:β4, and α3:β4:α5 cRNAs at the indicated ratios. Current amplitudes from 1:3 to 1:10 α3β4 combinations are significantly increased compared with 1:1 ratio (*$p < 0.05$; ***$p < 0.001$). Addition of α5 to the α3β4 complex leads to a significant decrease of current amplitudes when equal amounts of β4 and α5 are injected (**$p < 0.01$ for Wt α5; ***$p < 0.001$ for α5 D397N). The D397N variant shows significantly stronger competition with β4 compared with Wt α5 (*$p < 0.05$). Triangles indicate increasing relative amounts of one specified subunit. ***B***, Representative traces of two-electrode voltage–clamp recordings. ***C***, Schematic representation of β2/β4 chimeras indicating the domains, motifs, or residues exchanged between β4 (green) and β2 (black) subunits and corresponding amino-acid number and substitutions (left). Fold current increase (right) indicates the relative current amplitude of nicotine-evoked currents for each β2/β4 chimera expressed with the α3 subunit at 1:10 relative to 1:1 ratio. All values are expressed as mean ± SEM; n = 5 per ratio in all experiments.

NOTES

Transgenic mice of the* Chrnb4/a3/a5 *gene cluster (Tabac mice)

To test the hypothesis that β4 is rate-limiting for nAChR assembly and function *in vivo* and that overexpression of β4 can strongly influence nicotine-evoked currents and behavioral responses to nicotine, we characterized a bacterial artificial chromosome (BAC) transgenic line spanning the *Chrnb4–Chrna3–Chrna5* gene cluster (Gong et al., 2003). The BAC transgene included the intact coding sequences of the *Chrnb4* gene, modified sequences of *Chrna3*, and incomplete sequences of *Chrna5*. *Chrna3* was modified by insertion of an enhanced green fluorescent protein (eGFP) cassette, followed by polyadenylation signals at the ATG translation initiator codon of *Chrna3* (Fig. 2A). The upstream sequences of *Chrna5*, encoding exon 1 splice variants (Flora et al., 2000), are missing in the BAC transgene (Fig. 2A). To promote correct expression of *Chrnb4*, the BAC included the intergenic and 5' flanking regions encompassing the *cis*-regulatory elements that coordinate cotranscriptional control of the genes in the cluster (Bigger et al., 1997; Xu et al., 2006; Medel and Gardner, 2007).

As a result of these modifications in the BAC transgene, these mice (referred to as Tabac mice for Transgenic a3b4a5 cluster) express high levels of β4

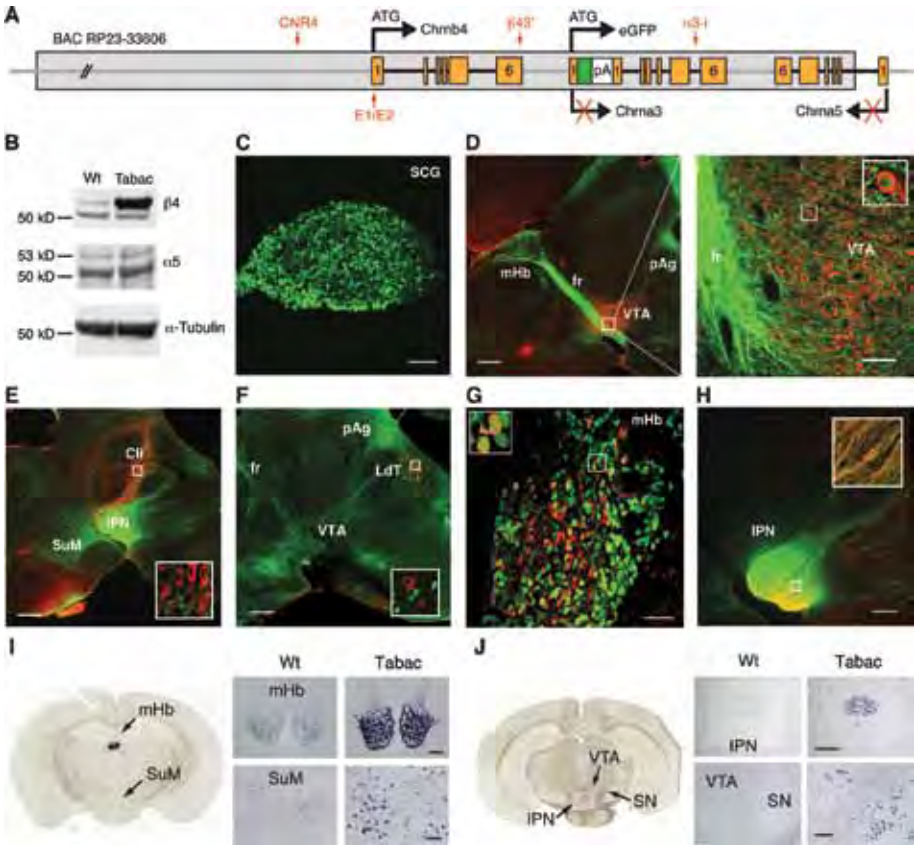

Figure 2. Tabac mice express elevated *Chrnb4* transcripts in *Chrna3*-eGFP labeled neurons. ***A***, Scheme of the modified mouse BAC containing the *Chrnb4–Chrna3–Chrna5* gene cluster. Yellow boxes, exons; green box, eGFP cassette; white box, polyadenylation signal (pA); black arrows, direction of transcription; red crosses, truncated transcription; *cis*-regulatory elements marked in red; CNR4, conserved noncoding region; β43' enhancer (Xu et al., 2006); E1/E2, SP1, and SP3 binding sites (Bigger et al., 1997); α3-i, transcriptional silencer (Medel and Gardner, 2007). ***B***, Western blot analyses of β4 (53 kD), α5 (2 splice variants: 50 kD and 53 kD), and α-Tubulin in brain extracts of Wt and Tabac mice. ***C–H***, eGFP-expressing neurons (green) in peripheral SCG (***C***) and in sagittal brain sections (except ***G***, coronal) of Tabac mice immunostained with TH (***D*** and ***E***) and ChAT (***F–H***) in red. ***I***, ***J***, *In situ* hybridization of *Chrnb4* transcripts in Wt and Tabac brain sections. fr, fasciculus retroflexus; LdT, laterodorsal tegmentum; pAg, periaqueductal gray; SCG, superior cervical ganglia; SN, substantia nigra. Scale bars: ***C***, 100 μm; ***D–F,*** 500 μm (magnification of ***D*** is indicated by the dotted lines; scale bar, 50 μm); ***G***, 50 μm; ***H***, 250 μm; mHb, 100 μm; SuM, 50 μm; IPN, 250 μm; VTA, 100 μm.

but not α5 (Fig 2*B*), and expression of α3 is replaced by expression of an eGFP reporter cassette to monitor the sites expressing the transgene (Fig. 2*C–H*). As shown in Figure 2, neurons expressing eGFP were evident in autonomic ganglia (Fig. 2*C*) and in very restricted brain structures (Figs. 2*D–H*) known to express these genes (Zoli et al., 1995). Immunostaining with cholinergic (choline acetyltransferase [ChAT]) and dopaminergic (tyrosine hydroxylase [TH]) markers indicated high expression of *Chrna3*/eGFP in cholinergic neurons of the Hb–IPN system (Fig. 2*G*,*H*). Intense *Chrna3*/eGFP expression was also detected in other brain areas (Fig. 3*D*,*E*) involved in nicotine addiction, such as the ventral tegmental area (VTA), the caudal linear nucleus (Cli), the supramammilary nucleus (SuM) (Ikemoto et al., 2006), and the laterodorsal tegmental nucleus (Fig. 2*F*), which provides modulatory input to the VTA (Maskos, 2008).

We performed *in situ* hybridization experiments to verify that the BAC accurately directed expression of transgenic *Chrnb4* transcripts to eGFP-positive brain areas. Tabac mice showed a prominent enrichment of *Chrnb4* transcripts in α3β4*-positive areas such as the mHb and IPN, and in brain areas that have been shown to express lower levels of *Chrnb4*, such as SuM (Dineley-Miller and Patrick, 1992) and VTA (Yang et al., 2009) (Fig. 2*I*,*J*). Reverse transcriptase (RT)–PCR studies showed that *Chrna4*, *Chrna7*, and *Chrnb2* transcripts (which are not present in the BAC) are not altered in Tabac mice (data not shown). Taken together, these data show that Tabac mice express high levels of β4, but not α5, in α3/eGFP–labeled cells in CNS and PNS structures known to express the *Chrnb4–Chrna3–Chrna5* nicotinic gene cluster. Thus, they provide a useful mouse model to test the consequences of enhanced β4 expression at endogenous sites.

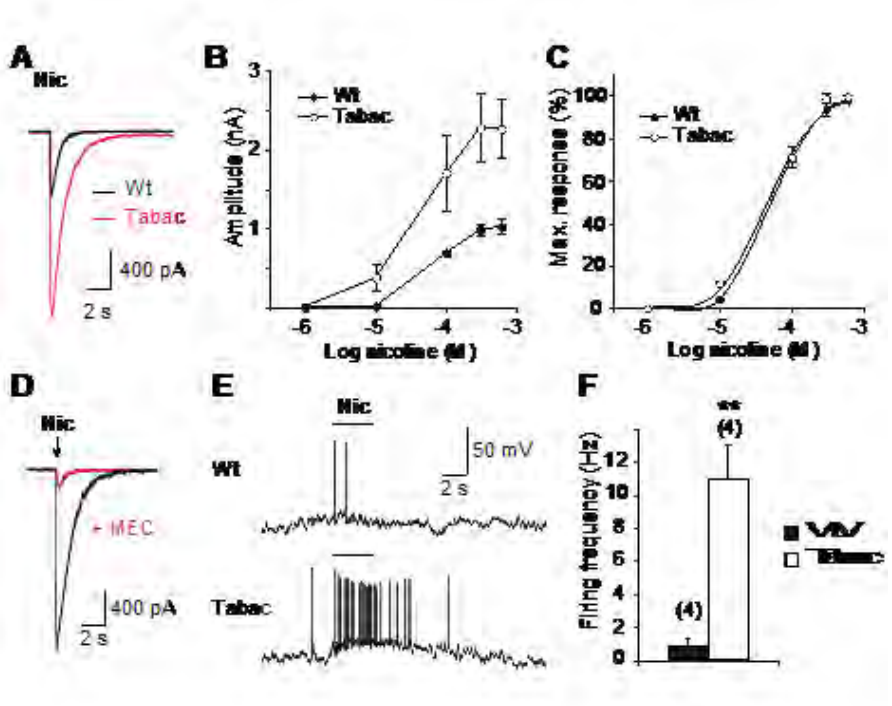

Figure 3. Tabac mice show increased α3β4* nAChR nicotine-evoked currents and firing frequency in *Chrna3*-eGFP–labeled neurons. ***A–F***, Whole-cell patch–clamp recordings of mHb neurons in acute brain slices from Wt and Tabac mice. Representative traces of nicotine-evoked currents (***A***, 100 μM, 50 ms application) and corresponding concentration-response relationships (***B***, peak amplitudes ± SEM; $n = 5–8$ cells per genotype; $p < 0.05$ by 2-way ANOVA). Dose-response curves in ***C*** were calculated relative to the maximal response to nicotine from ***B***. ***D***, Mecamylamine (MEC) (3 μM, 3 min) inhibition of nicotine-evoked currents in neurons of Tabac mice. Representative current–clamp recordings (***E***) and quantification of action potentials upon local application of nicotine (1 μM, 3 s) in neurons of Wt and Tabac mice (***F***, mean firing frequency ± SEM; $n = 4$; $p < 0.01$). Numbers in parentheses represent number of neurons tested. All values expressed as mean ± SEM.

NOTES

Increased nicotine-evoked currents in transgenic Tabac mice

Given the demonstration that the level of β4 expression is rate-limiting for the function of α3β4α5 receptors *in vitro* (Fig. 1), we were next interested in determining whether enhanced expression of *Chrnb4* in Tabac neurons resulted in elevated nicotine-evoked currents *in vivo*. Previous studies have shown that neurons in the mHb express high levels of α3β4α5 receptors (Quick et al., 1999). Accordingly, we employed patch–clamp recordings to measure nicotine-evoked currents in mHb neurons of Tabac mice. A large proportion of mHb neurons in Wt mice ($n = 20$ of $N = 23$ neurons recorded) responded to local fast application (50 ms) of nicotine (Fig. 4*A*,*B*). In *Chrna3*/eGFP–labeled mHb neurons of Tabac mice, nicotine elicited significantly increased peak currents in comparison with Wt littermates (on average, 3.4-fold at 100 μM nicotine, two-way ANOVA $p < 0.05$) (Fig. 3*B*). Similarly increased responses were obtained using acetylcholine (ACh) (data not shown). Dose-response curves for nicotine showed no significant differences between Wt and Tabac mice, indicating that the affinity of the receptors in the transgenic mice is not altered (Fig 3C). Application of mecamylamine, a nonselective potent inhibitor of α4β2* and α3β4* nAChRs (Bacher et al., 2009), resulted in a blockade of as much as 90% of the nicotine-elicited responses in Tabac mice (Fig. 3*D*). This finding demonstrates that the enhanced nicotine responses in Tabac neurons result directly from elevated levels of functional nAChRs.

To determine whether these additional receptors cause enhanced neuronal excitability, the firing rate of habenular neurons was measured in current–clamp assays in response to nicotine. Neurons from Wt and Tabac mice were silent at rest (–70 mV). Local nicotine application (1 μM for 3 s) elicited single action potentials in Wt neurons, whereas nicotine induced a robust burst of action potentials with a 13-fold higher firing frequency on average in Tabac neurons ($p < 0.005$) (Fig. 4*E*,*F*). Together, these results indicate that the increased sensitivity of mHb neurons to nicotine in Tabac mice results from the presence of additional functional nAChRs rather than from changes in the nicotine affinity of existing receptors.

Tabac mice show strong aversion to nicotine consumption, and display nicotine-conditioned place aversion

We were next interested in the effects of elevated nAChR expression on the behavioral responses of Tabac mice to nicotine. Measurements of drinking volumes showed that Tabac mice consumed significantly less nicotine-containing water than Wt littermates (Fig. 4*A*,*B*). Because nicotine solutions have a bitter taste, nicotine was diluted in saccharin solution, and control experiments with a bitter solution (containing quinine) were performed. There were no differences in consumption of regular, sweetened, or bitter water between the two groups (Fig. 4*A*).

Next, we performed a free-choice consumption experiment in which mice were allowed to choose between regular water and water supplemented with different concentrations of nicotine (1–100 μg/ml) without saccharin. Analysis of the nicotine volume consumed relative to the total fluid intake (Fig. 4C) indicated that Tabac mice significantly avoided drinking nicotine solutions containing more than 5 μg/ml nicotine ($p < 0.05$; two-way ANOVA), while Wt showed no preference between water and nicotine solutions below 50 μg/ml and avoided drinking the highest concentration of nicotine solution tested. It is possible that the decrease in drinking resulted from the negative consequences of hyperactivation of the autonomic nervous system, leading to gastric distress or nausea. However, we observed no significant differences in body weight (Fig. 4*D*), micturition, and digestion before and during the nicotine consumption experiments.

As an independent measure of the effects of nicotine in Tabac mice, conditioned place aversion (CPA) assays were performed. Because conditioning to nicotine is dependent on both concentration and strain (O'Dell and Khroyan, 2009), we measured CPA in Wt C57BL/6 littermates at 0.5 mg nicotine/kg body weight. Under these conditions, we observed neither a preference for nor an aversion to nicotine. In contrast, strong conditioned place aversion to nicotine was observed in Tabac mice (Fig. 4*E*). These data both confirm the conclusions of the nicotine consumption assays and demonstrate that negative reward learning associated to nicotine is strongly increased in Tabac mice. We conclude that overexpression of the β4 subunit *in vivo* leads to an increase in functional α3β4* receptors, resulting in a higher sensitivity to the aversive properties of nicotine.

Lentiviral-mediated expression of the α5 D397N variant in the medial habenula reverses nicotine aversion in Tabac mice

Our observations showed that the α5 D397N variant reduces α3β4α5 nicotine-evoked currents in oocytes (Fig. 1) and that the mHb contains a high density of native α5 nAChR subunits in combination with α3β4 subunits (Fig. 2). They suggested that the enhanced nicotine aversion evident in Tabac mice could be

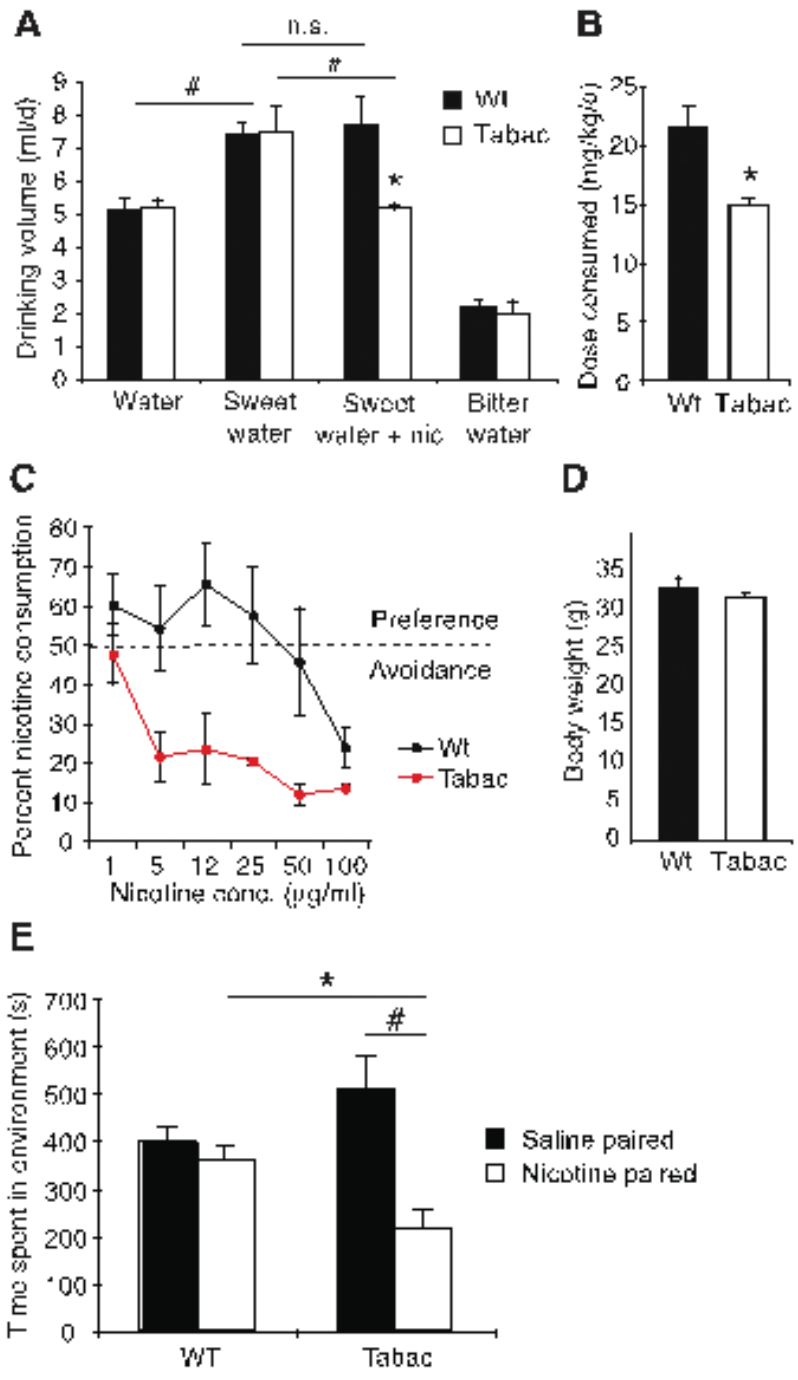

Figure 4. Tabac mice consume less nicotine and show conditioned place aversion. ***A***, ***B***, Nicotine consumption in a no-choice paradigm (1 drinking bottle). ***A***, Drinking volumes (ml/mouse/day) of water, sweet water (2% saccharine), and bitter water (5 mM quinine). The tested period of consumption was 3 d (paired t test; $p < 0.05$). ***B***, The dose of nicotine consumed expressed as the mg of nicotine consumed per day considering the body weight of the mouse (mg/kg/d) ($p < 0.05$). Wt mice ($n = 10$); Tabac mice ($n = 10$). ***C***, Nicotine consumption in a two-bottle-choice paradigm between water and water containing the indicated nicotine concentrations, expressed as percent of the volume of nicotine solution consumed divided by the total fluid intake and per day. Each concentration was tested for 3 d. Dashed line at 50% indicates no preference. Wt mice ($n = 7$); Tabac mice ($n = 6$); two-way ANOVA; $p < 0.05$. ***D***, Body weight of Wt and Tabac mice after nicotine drinking tests. ***E***, Nicotine administration (0.5 mg/kg) elicits place aversion to nicotine-paired environment in Tabac mice. Following conditioning, Tabac mice preferred the saline-paired environment over the nicotine-paired environment (paired *t* test; $p < 0.05$). Wt mice spent significantly more time in the nicotine-paired environment compared with Tabac mice (*$p < 0.05$). Wt mice ($n = 7$); Tabac mice ($n = 6$). Data are expressed as time spent in drug-paired environments after drug conditioning. All values are expressed as mean ± SEM.

NOTES

reversed by expression of the α5 variant in the mHb. To test this hypothesis, we employed lentiviral vector–mediated transduction to express the α5 D397N in mHb neurons of Tabac mice. We bilaterally injected either control lentivirus (LV-PC) or the LV-α5 D397N (LV-α5N) viruses in Tabac mice. As shown in Figure 5*B*, immunostaining for the mCHERRY reporter of LV-α5N expression or direct fluorescence derived from the control LV demonstrated that the lentiviral-transduced area corresponds with that occupied by α3β4*-eGFP–labeled neurons in the mHb of Tabac mice.

Given that the maximal difference in nicotine consumption in Tabac mice occurred at 25 μg/ml nicotine (Fig. 5C), mice were again given a two-bottle choice test to measure nicotine aversion. These experiments were performed in Tabac mice backcrossed to the inbred mouse line C57/BL6 (Fig. 5C), which has been shown to have a high basal level of self-selection of nicotine (Meliska et al., 1995; Robinson et al., 1996; Glatt et al., 2009), and in Tabac mice outbred between FBV/N mixed and Swiss Webster (Fig. 5*D*). As shown in Figure 5C, in C57/BL6 Tabac mice, injection of the LV-α5N virus reversed their nicotine aversion compared with mice injected with the control virus. In outbred Tabac mice, we observed no alteration in nicotine aversion in Tabac mice injected with the control virus (Fig. 5*D*) with respect to uninjected Tabac mice (Fig. 5C). Importantly, infection with LV-α5N virus reversed nicotine aversion in Tabac mice (Fig. 5*D*), restoring nicotine consumption in α5D397N-

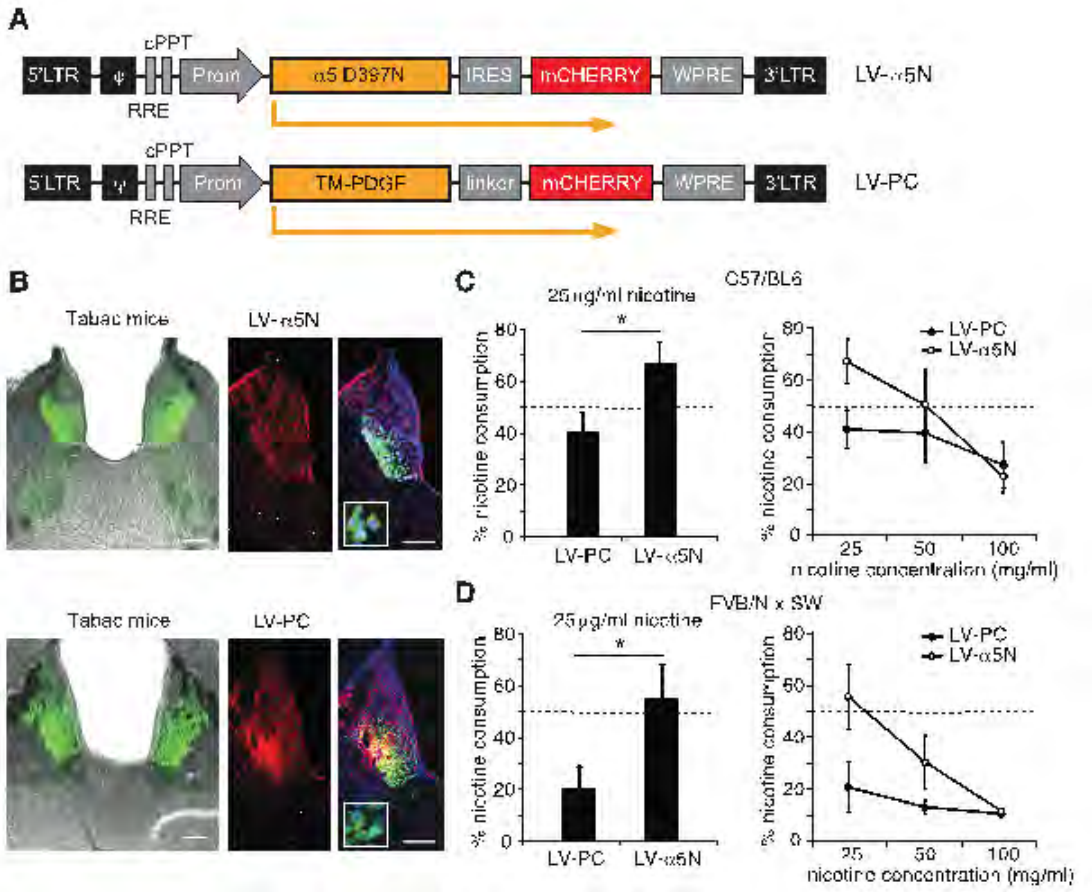

Figure 5. Reversal of nicotine aversion in Tabac mice by lentiviral vector–mediated expression of the α5 D397N variant in the mHb. ***A***, Schematic representation of the lentiviral (LV) constructs used for brain stereotactic injections. LV-α5N carries the mouse α5 variant D397N followed by an IRES and the mCHERRY reporter. The control virus (LV-PC) carries mCHERRY fused to the N-terminus of the transmembrane domain of the platelet-derived growth factor receptor (TM-PDGF) via a linker domain. ***B***, Coronal brain sections of Tabac mice stereotactically injected in the mHb with the indicated lentivirus. Colocalization of eGFP fluorescence driven by the transgene in Tabac mice and mCHERRY red fluorescence for LV-PC, or mCHERRY immunofluorescence for mice injected with LV-α5N. Two-bottle choice nicotine consumption in Tabac mice after stereotactic bilateral injection of control (LV-PC) and mutated α5 (LV-α5N) lentiviral constructs in the mHb. Tabac mice backcrossed to C57BL6; $n = 4$ for LV-PC; $n = 5$ for LV-α5N; $p < 0.05$ (C) and Tabac mice hybrid of FVB/N and Swiss Webster; $n = 8$ for LV-PC; $n = 9$ for LV-α5N (D). IRES, internal ribosomal entry site; LTR, long terminal repeat; WPRE, woodchuck postregulatory element. Scale bars: ***B, C, D***, 100 μm.

infected Tabac mice to levels evident in Wt mice (Fig. 5C). These results demonstrate a major role for the mHb in nicotine consumption.

Discussion

Human genetic studies have established an association between the *Chrnb4–CHRNA3–CHRNA5* locus and tobacco use (Thorgeirsson et al., 2008; Weiss et al., 2008; Saccone et al., 2009; Amos et al., 2010b). Here we report a novel mouse model (Tabac mice) with altered nicotine consumption and conditioned place aversion caused by elevated levels of β4, enhanced nicotine-evoked currents, and increased surface expression of functional nAChRs at endogenous sites. The ability of β4 to enhance nicotine-evoked currents depends on a single critical residue (S435) located in the intracellular vestibule of the receptor. Interestingly, modeling studies revealed that one of the most common SNPs associated with tobacco usage, D398N in the α5 subunit, also maps to this domain. Functional analyses of this variant demonstrate that alterations in this domain can result in profound effects on nicotine-evoked currents. Based on our studies in Tabac mice in which enhanced current is associated with increased aversion to nicotine, we predicted that the α5 variant (corresponding to D397N in mice) should increase nicotine consumption consistent with its association with smoking. To test this idea, and given that the mHb contains a very high concentration of endogenous α3β4α5 receptors, as well as elevated levels of β4 driven by the Tabac transgene, we introduced the α5 variant by viral-mediated transduction in habenular neurons of Tabac mice. The reversal of the nicotine aversion achieved in Tabac mice observed in these experiments demonstrates that the mHb plays a major regulatory role in nicotine consumption.

Three main points are addressed in this study. First, changes both in the coordinated expression of α3β4α5 subunits (i.e., overexpression of the β4 subunit) as well as in single residues (i.e., *in vivo* viral-mediated expression of the α5 D397N variant) have a strong influence on nicotine consumption in mice. This is consistent with recent genome-wide association studies that have identified SNPs in both regulatory and coding regions of the *Chrnb4–CHRNA3–CHRNA5* gene cluster that are associated with nicotine dependence (Levitin et al., 2008; Thorgeirsson et al., 2008; Saccone et al., 2009). Thus, our studies provide a new model for further exploration of the involvement of α3β4α5 nAChR function in nicotine consumption.

Second, our studies demonstrate that the intracellular vestibule of the α3β4α5 receptor exerts an important effect on nicotine-evoked currents. The high concentration of charges in this membrane-associated domain is conserved in the superfamily of Cys-loop receptors (Kelley et al., 2003; Unwin, 2005; Carland et al., 2009). Electrostatic calculations by homology with the *Torpedo* nAChR predict that α3β4α5 receptors form a highly electronegative vestibule most likely to promote a stabilizing environment for cation outflow. The change in current amplitude produced by substitutions of charged residues (S435R and D397N) in this domain of the receptor predicts that alterations of the electrostatic charge of the vestibule are critical for receptor function. This finding is consistent with studies of the inner vestibule in other Cys-loop receptor channels. For example, in 5HT3A receptors, the substitution of arginine-positive residues increased channel conductance, whereas introduction of basic residues in this domain of α1 glycine receptors decreases glycine-evoked currents (Kelley et al., 2003; Carland et al., 2009). Numerous reports have linked the α5 D398N polymorphism to smoking incidence (Saccone et al., 2009; Bierut, 2008, 2010). Incorporation of D398N α5 variant into α4β2-containing receptors in transfected cells results in a twofold reduction in epibatidine-evoked calcium currents without a change in surface expression (Bierut et al., 2008), consistent with the reduction in nicotine-evoked current amplitudes reported here upon incorporation of this variant into α3β4 containing nAChRs.

Taken together, these observations support the hypothesis that substitution of this charged residue modifies the vestibule electrostatic charge but not the number of receptors incorporated into the plasma membrane. In contrast, the increase in receptor-surface expression in Tabac mice and the identification of a single unique residue in the β4 subunit (S435R) suggest that the β4 subunit is rate-limiting for the formation of α3β4α5 nAChRs. S435R is essential for the increase of currents observed in this study upon overexpression of the β4 subunit; further, S435R can confer this property to β2 subunits. Although the precise role of S435 is not yet clear, it may be involved in stabilizing nAChR complexes, export of the receptors from the endoplasmic reticulum, interactions with trafficking proteins, or alterations in its turnover from the cell surface. For example, rapsyn binding to the α-helical domains corresponding to the inner vestibule of α1β1γδ nAChR is required for surface expression of this receptor (Lee et al., 2009). It also has been shown that binding of UBXD4 to the cytoplasmic loop of α3 can interfere with its ubiquitination and, consequently, the number of α3-containing receptors at the cell surface (Rezvani et al., 2010). Thus,

NOTES

NOTES

our studies point to two mechanisms mediated by specific residues in the inner vestibule: one leading to ion permeation changes within a single α3β4α5 receptor and the other leading to increased surface expression of receptors by native β4.

Third, the studies presented here demonstrate that the mHb has a major influence on the control of nicotine consumption. These studies extend the findings from previous studies on the role of the habenula in nicotine withdrawal and drug addiction (Taraschenko et al., 2007; Jackson et al., 2008; Salas et al., 2004, 2009) and, recently, in nicotine self-administration (Fowler et al., 2011). Although multiple interconnected brain regions, including the prefrontal cortex, VTA, thalamus, striatum, and amygdala, are affected by chronic use of nicotine, the habenular system is emerging as an important station in pathways regulating the behavioral effects of nicotine (Rose, 2007; De Biasi and Salas, 2008; Changeux, 2010). The mHb projects mainly to the IPN, which, in turn, seems to inhibit the motivational response to nicotine intake. Thus, inactivation of the mHb and IPN both result in increased intake of nicotine (Fowler et al., 2011). Consistent with these studies, overexpression of β4 results in enhanced activity of the mHb, resulting in the opposing effect: aversion to nicotine. Reversal of nicotine aversion in Tabac mice overexpressing β4 is achieved by expression of the α5 D397N in mHb neurons. Similarly, α5 re-expression in the habenula of α5 KO mice normalizes their nicotine intake (Fowler et al., 2011).

Taken together, these studies provide direct evidence that the mHb acts as a gatekeeper in the control of nicotine consumption and that the balanced contribution of β4 and α5 subunits is critical for this function. Further analyses of nAChR function in the habenulo-IPN tract and its associated circuitry will be required to fully understand the addictive properties of nicotine.

References

Amos CI, Gorlov IP, Dong Q, Wu X, Zhang H, Lu EY, Scheet P, Greisinger AJ, Mills GB, Spitz MR (2010a) Nicotinic acetylcholine receptor region on chromosome 15q25 and lung cancer risk among African Americans: a case-control study. J Natl Cancer Inst 102:1199-1205.

Amos CI, Spitz MR, Cinciripini P (2010b) Chipping away at the genetics of smoking behavior. Nat Genet 42:366-368.

Bacher I, Wu B, Shytle DR, George TP (2009) Mecamylamine—a nicotinic acetylcholine receptor antagonist with potential for the treatment of neuropsychiatric disorders. Expert Opin Pharmacother 10:2709-2721.

Bierut LJ (2010) Convergence of genetic findings for nicotine dependence and smoking related diseases with chromosome 15q24-25. Trends Pharmacol Sci 31 46-51.

Bierut LJ, Stitzel JA, Wang JC, Hinrichs AL, Grucza RA, Xuei X, Saccone NL, Saccone SF, Bertelsen S, Fox L, Horton WJ, Breslau N, Budde J, Cloninger CR, Dick DM, Foroud T, Hatsukami D, Hesselbrock V, Johnson EO, Kramer J, et al. (2008) Variants in nicotinic receptors and risk for nicotine dependence. Am J Psychiatry 165:1163-1171.

Bigger CB, Melnikova IN, Gardner PD (1997) Sp1 and Sp3 regulate expression of the neuronal nicotinic acetylcholine receptor beta4 subunit gene. J Biol Chem 272:25976-25982.

Carland JE, Cooper MA, Sugiharto S, Jeong HJ, Lewis TM, Barry PH, Peters JA, Lambert JJ, Moorhouse AJ (2009) Characterization of the effects of charged residues in the intracellular loop on ion permeation in α1 glycine receptor channels. J Biol Chem 284:2023-2030.

Changeux JP (2010) Nicotine addiction and nicotinic receptors: lessons from genetically modified mice. Nat Rev Neurosci 11:389-401.

Dani JA, Heinemann S (1996) Molecular and cellular aspects of nicotine abuse. Neuron 16:905-908.

De Biasi M, Salas R (2008) Influence of neuronal nicotinic receptors over nicotine addiction and withdrawal. Exp Biol Med (Maywood) 233:917-929.

Dineley-Miller K, Patrick J (1992) Gene transcripts for the nicotinic acetylcholine receptor subunit, beta4, are distributed in multiple areas of the rat central nervous system. Brain Res Mol Brain Res 16:339-344.

Flora A, Schulz R, Benfante R, Battaglioli E, Terzano S, Clementi F, Fornasari D (2000) Transcriptional regulation of the human α5 nicotinic receptor subunit gene in neuronal and non-neuronal tissues. Eur J Pharmacol 393:85-95.

Fowler CD, Lu Q, Johnson PM, Marks MJ, Kenny PJ (2011) Habenular α5 nicotinic receptor subunit signalling controls nicotine intake. Nature 471:597-601.

Gahring LC, Rogers SW (2010) Nicotinic receptor subunit α5 modifies assembly, up-regulation, and response to pro-inflammatory cytokines. J Biol Chem 28526049-26057.

NOTES

Glatt AR, Denton K, Boughter JD Jr (2009) Variation in nicotine consumption in inbred mice is not linked to orosensory ability. Chem Senses 34:27-35.

Gong S, Zheng C, Doughty ML, Losos K, Didkovsky N, Schambra UB, Nowak NJ, Joyner A, Leblanc G, Hatten ME, Heintz N (2003) A gene expression atlas of the central nervous system based on bacterial artificial chromosomes. Nature 425:917-925.

Gotti C, Clementi F, Fornari A, Gaimarri A, Guiducci S, Manfredi I, Moretti M, Pedrazzi P, Pucci L, Zoli M (2009) Structural and functional diversity of native brain neuronal nicotinic receptors. Biochem Pharmacol 78:703-711.

Ikemoto S, Qin M, Liu ZH (2006) Primary reinforcing effects of nicotine are triggered from multiple regions both inside and outside the ventral tegmental area. J Neurosci 26:723-730.

Jackson KJ, Martin BR, Changeux JP, Damaj MI (2008) Differential role of nicotinic acetylcholine receptor subunits in physical and affective nicotine withdrawal signs. J Pharmacol Exp Ther 325:302-312.

Kedmi M, Beaudet AL, Orr-Urtreger A (2004) Mice lacking neuronal nicotinic acetylcholine receptor beta4-subunit and mice lacking both α5- and β4-subunits are highly resistant to nicotine-induced seizures. Physiol Genomics 17:221-229.

Kelley SP, Dunlop JI, Kirkness EF, Lambert JJ, Peters JA (2003) A cytoplasmic region determines single-channel conductance in 5-HT_3 receptors. Nature 424:321-324.

Lee Y, Rudell J, Ferns M (2009) Rapsyn interacts with the muscle acetylcholine receptor via alpha-helical domains in the alpha, beta, and epsilon subunit intracellular loops. Neuroscience 163:222-232.

Levitin F, Weiss M, Hahn Y, Stern O, Papke RL, Matusik R, Nandana SR, Ziv R, Pichinuk E, Salame S, Bera T, Vincent J, Lee B, Pastan I, Wreschner DH (2008) *PATE* gene clusters code for multiple, secreted TFP/Ly-6/uPAR proteins that are expressed in reproductive and neuron-rich tissues and possess neuromodulatory activity. J Biol Chem 283:16928-16939.

Lu B, Su Y, Das S, Wang H, Wang Y, Liu J, Ren D (2009) Peptide neurotransmitters activate a cation channel complex of NALCN and UNC-80. Nature 457:741-744.

Maskos U (2008) The cholinergic mesopontine tegmentum is a relatively neglected nicotinic master modulator of the dopaminergic system: relevance to drugs of abuse and pathology. Br J Pharmacol 153(Suppl 1):S438-S445.

Maskos U, Molles BE, Pons S, Besson M, Guiard BP, Guilloux JP, Evrard A, Cazala P, Cormier A, Mameli-Engvall M, Dufour N, Cloëz-Tayarani I, Bemelmans AP, Mallet J, Gardier AM, David V, Faure P, Granon S, Changeux JP (2005) Nicotine reinforcement and cognition restored by targeted expression of nicotinic receptors. Nature 436:103-107.

McGehee DS, Role LW (1995) Physiological diversity of nicotinic acetylcholine receptors expressed by vertebrate neurons. Annu Rev Physiol 57:521-546.

Medel YF, Gardner PD (2007) Transcriptional repression by a conserved intronic sequence in the nicotinic receptor α3 subunit gene. J Biol Chem 282:19062-19070.

Meliska CJ, Bartke A, McGlacken G, Jensen RA (1995) Ethanol, nicotine, amphetamine, and aspartame consumption and preferences in C57BL/6 and DBA/2 mice. Pharmacol Biochem Behav 50:619-626.

Nashmi R, Dickinson ME, McKinney S, Jareb M, Labarca C, Fraser SE, Lester HA (2003) Assembly of α4β2 nicotinic acetylcholine receptors assessed with functional fluorescently labeled subunits: effects of localization, trafficking, and nicotine-induced upregulation in clonal mammalian cells and in cultured midbrain neurons. J Neurosci 23:11554-11567.

O'Dell LE, Khroyan TV (2009) Rodent models of nicotine reward: what do they tell us about tobacco abuse in humans? Pharmacol Biochem Behav 91:481-488.

Picciotto MR (1998) Common aspects of the action of nicotine and other drugs of abuse. Drug Alcohol Depend 51:165-172.

Quick MW, Ceballos RM, Kasten M, McIntosh JM, Lester RA (1999) α3β4 subunit-containing nicotinic receptors dominate function in rat medial habenula neurons. Neuropharmacology 38:769-783.

Ren XQ, Cheng SB, Treuil MW, Mukherjee J, Rao J, Braunewell KH, Lindstrom JM, Anand R (2005) Structural determinants of α4β2 nicotinic acetylcholine receptor trafficking. J Neurosci 25:6676-6686.

NOTES

Rezvani K, Teng Y, De Biasi M (2010) The ubiquitin-proteasome system regulates the stability of neuronal nicotinic acetylcholine receptors. J Mol Neurosci 40:177-184.

Robinson SF, Marks MJ, Collins AC (1996) Inbred mouse strains vary in oral self-selection of nicotine. Psychopharmacology (Berl) 124:332-339.

Rose JE (2007) Multiple brain pathways and receptors underlying tobacco addiction. Biochem Pharmacol 74:1263-1270.

Saccone NL, Wang JC, Breslau N, Johnson EO, Hatsukami D, Saccone SF, Grucza RA, Sun L, Duan W, Budde J, Culverhouse RC, Fox L, Hinrichs AL, Steinbach JH, Wu M, Rice JP, Goate AM, Bierut LJ (2009) The *CHRNA5–CHRNA3–Chrnb4* nicotinic receptor subunit gene cluster affects risk for nicotine dependence in African-Americans and in European-Americans. Cancer Res 69:6848-6856.

Salas R, Pieri F, De Biasi M (2004) Decreased signs of nicotine withdrawal in mice null for the β4 nicotinic acetylcholine receptor subunit. J Neurosci 24:10035-10039.

Salas R, Sturm R, Boulter J, De Biasi M (2009) Nicotinic receptors in the habenulo-interpeduncular system are necessary for nicotine withdrawal in mice. J Neurosci 29:3014-3018.

Scofield MD, Tapper AR, Gardner PD (2010) A transcriptional regulatory element critical for *Chrnb4* promoter activity *in vivo*. Neuroscience 170:1056-1064.

Tapper AR, McKinney SL, Nashmi R, Schwarz J, Deshpande P, Labarca C, Whiteaker P, Marks MJ, Collins AC, Lester HA (2004) Nicotine activation of α4* receptors: sufficient for reward, tolerance, and sensitization. Science 306:1029-1032.

Taraschenko OD, Shulan JM, Maisonneuve IM, Glick SD (2007) 18-MC acts in the medial habenula and interpeduncular nucleus to attenuate dopamine sensitization to morphine in the nucleus accumbens. Synapse 61:547-560.

Thorgeirsson TE, Geller F, Sulem P, Rafnar T, Wiste A, Magnusson KP, Manolescu A, Thorleifsson G, Stefansson H, Ingason A, Stacey SN, Bergthorsson JT, Thorlacius S, Gudmundsson J, Jonsson T, Jakobsdottir M, Saemundsdottir J, Olafsdottir O, Gudmundsson LJ, Bjornsdottir G, et al. (2008) A variant associated with nicotine dependence, lung cancer and peripheral arterial disease. Nature 452:638-642.

Unwin N (2005) Refined structure of the nicotinic acetylcholine receptor at 4A resolution. J Mol Biol 346:967-989.

Weiss RB, Baker TB, Cannon DS, von Niederhausern A, Dunn DM, Matsunami N, Singh NA, Baird L, Coon H, McMahon WM, Piper ME, Fiore MC, Scholand MB, Connett JE, Kanner RE, Gahring LC, Rogers SW, Hoidal JR, Leppert MF (2008) A candidate gene approach identifies the *CHRNA5-A3-B4* region as a risk factor for age-dependent nicotine addiction. PLoS Genet 4:e1000125.

Whiting PJ, Lindstrom JM (1988) Characterization of bovine and human neuronal nicotinic acetylcholine receptors using monoclonal antibodies. J Neurosci 8:3395-3404.

Xu W, Gelber S, Orr-Urtreger A, Armstrong D, Lewis RA, Ou CN, Patrick J, Role L, De Biasi M, Beaudet AL (1999) Megacystis, mydriasis, and ion channel defect in mice lacking the α3 neuronal nicotinic acetylcholine receptor. Proc Natl Acad Sci USA 96:5746-5751.

Xu X, Scott MM, Deneris ES (2006) Shared long-range regulatory elements coordinate expression of a gene cluster encoding nicotinic receptor heteromeric subtypes. Mol Cell Biol 26:5636-5649.

Yang K, Hu J, Lucero L, Liu Q, Zheng C, Zhen X, Jin G, Lukas RJ, Wu J (2009) Distinctive nicotinic acetylcholine receptor functional phenotypes of rat ventral tegmental area dopaminergic neurons. J Physiol 587:345-361.

Zoli M, Le Novere N, Hill JA Jr, Changeux JP (1995) Developmental regulation of nicotinic ACh receptor subunit mRNAs in the rat central and peripheral nervous systems. J Neurosci 15:1912-1939.